THE JOURNAL OF PHYSICAL CHEMISTRY B

ARTICLE

pubs.acs.org/JPCB

Solvent and Salt Effects on Structural Stability of Human Telomere

Yutaka Maruyama,[†] Taku Matsushita,[‡] Ryuichi Ueoka,[‡] and Fumio Hirata*[,†,§]

[†]Department of Theoretical Molecular Science, Institute for Molecular Science, Okazaki 444-8585, Japan

[‡]Graduate School of Engineering, Sojo University, Kumamoto, Japan

[§]Department of Functional Molecular Science, The Graduate University for Advanced Studies, Okazaki 444-8585, Japan

ABSTRACT: The free energy and the solvation structures of the G-quadruplex telomeric DNA in pure water and in the 0.1 M aqueous solutions of sodium and potassium chlorides are calculated on the basis of the 3D-RISM theory. To find the most stable structure of each G-quadruplex in the aqueous solutions, the free energy is minimized in the solutions on the basis of the quasi-Newton method using the analytical derivative of the solvation free energy obtained from 3D-RISM. In pure water, the chair-type conformation was found to be the most stable structure, which is followed by basket-, hybrid-, and propeller-type structures in the order. It is clarified that the order of the stability is determined essentially by the solvation free energy, not by the conformational energy. The order of the stability changes in 0.1 M NaCl solutions from that in pure water. The basket-type structure becomes the most stable one in the electrolyte solution. The theoretical finding is consistent with the experimental observation due to NMR. The reversed order of the conformational stability was attributed to the salt effect, especially, to that from the Na^+ ions bound at interstrand spaces of DNA. Concerning the conformational stability in KCl solutions, which has not been clarified yet by experiments, our results predict that the order is not changed from that in pure water; that is, the chair-type is the most stable one. The finding suggests that the effect of the potassium ion upon the structure is not so strong as the sodium ion to change the order of the stability determined in pure water. The result is consistent with our finding for RDFs of the ions bound at the interstrand spaces in DNA, which indicates clearly that the affinity of K^+ to the binding site is weaker than that of Na^+.

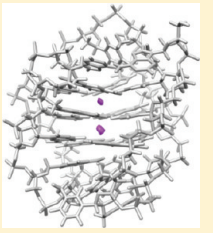

I. INTRODUCTION

Human telomere DNA has been attracting increasing attention because of its role in the biology of both cancer and aging.[1−3] The single-stranded telomere terminus can adopt the structure of a G-quadruplex, which is of particular importance for anticancer drug discovery.[4−14]

Various G-quadruplex structures of the 22 nt sequence d-[AGGG(TTAGGG)$_3$] have been reported.[15,16] The structure determined by NMR in aqueous solutions of sodium chloride (NaCl) is an antiparallel basket-type quadruplex.[17] However, the structure in aqueous solutions of potassium chloride (KCl) has not been determined yet and remains controversial. Although its structure in crystal has been reported, the structure is a parallel propeller-type G-quadruplex, which is different from that found in NaCl solutions.[18]

The solution structure in the presence of K^+ is of particular interest, as the intracellular K^+ concentration is higher than that of Na^+. Recently, several groups have reported the (3+1) hybrid-type G-quadruplex in physiological solution of potassium chloride.[19−24] One of these studies based on the circular dichlorism (CD) and NMR is concerned with the structure and the thermal stability of a series of systematic derivatives of telomeric DNA in which guanosines were substituted with 8-bromoguanosines.[25−28] The study allowed us to determine the syn/anti conformational preference of each guanosine in the naturally occurring structure, which helped to suggest a fold of the molecule. However, the difference in the syn/anti conformation of guanosine between the chair- and hybrid-type telomeres is small as is seen in Table 1. The difference is observed in only one guanosine conformation, which is located in the second position of the 5′ end of the GGG, indicated by mesh background. Thus, the telomeric DNA forming the hybrid-type structure, in which guanosines are substituted by 8-bromoguanosines, may also form the chair-type structure. In fact, using ^{125}I-radioprobing, Panyutin et al. suggested that a chair-type G-quadruplex might coexist in aqueous solutions of KCl.[29] Sugiyama et al. also showed on the basis of the CD spectroscopy that a mixture of hybrid- and chair-type G-quadruplexes exists in aqueous solutions of KCl.[25] Taylor et al. indicated that an interloop thymine photodimer formation in telomere, which cannot arise from the hybrid-type structure, occurs under the UVB light in the presence of K^+.[30] These results indicate that the chair-type structure is also possible in aqueous solutions of KCl. Bombard et al. concluded that human telomere d[AGGG(TTAGGG)$_3$] formed the basket-type structure in K^+ solution by the cross-linking of adenines and guanines, but their results can be interpreted by the chair-type model, too.[31]

Some computer simulation studies have been reported as complementary to the NMR experiments.[32−35] Molecular dynamics simulations of binding the specific ligand to the G-quadruplex have been performed.[36] Boyd et al. studied the electronic property and the structural stability of a basket-type G-quadruplex

Received: October 7, 2010
Revised: January 19, 2011
Published: February 18, 2011

Table 1. Sequence of Telomeric DNA and Guanosine Conformations of Hybrid and Chair Type[a]

	A	G	G	G	T	T	A	G	G	G	T	T	A	G	G	G	T	T	A	G	G	G
hybrid		S	A	A				S	A	A				S	S	A				S	A	A
chair		S	S	A				S	A	A				S	S	A				S	A	A

[a] S and A indicate syn and anti conformations of each guanosine.

in water.[37] However, the results are far from conclusive, because they ignore the effect of environmental electrolyte solution, which undoubtedly plays a crucial role to determine the G-quadruplex structure.

In the present paper, we report an analysis for the conformational stability and the solvation structure of telomeric DNA based on the three-dimensional reference interaction site model (3D-RISM) theory.[38] In the study, we put a particular stress on the specificity of electrolytes to determine the telomere structure. We first examine the conformational stability and the solvation structure of telomeric DNA in NaCl solutions to see if the theory is capable of reproducing the solution structure of DNA determined by NMR. We then apply the same method to predict the most stable conformation of telomeric DNA in KCl solutions, which has not been determined yet by experimental methods.

The method (3D-RISM) used in the present study has an extraordinary capability to explore the configuration space of aqueous solutions of biomlecules, because it performs the configuration integral analytically over the entire system, which includes an infinitely large number of molecules in solution. The method treats solvent and ion configurations microscopically in terms of a probabilistic distribution, so that it is capable of "detecting" the distribution of ions recognized by the binding site in telomeric DNA just as the X-ray crystallography does. The method has been applied successfully to a number of problems in biophysics and chemistry to describe the solvation phenomena as well as the molecular recognition of biomolecules in solutions.[39−44] In particular, the robustness of the method is demonstrated recently by comparing the solvation structure of DNA calculated from the theory with that from the molecular dynamics simulation.[45] In addition, the study with 3D-RISM theory reproduced DNA B-Z transition and clarified its physical origin.[46] In the present study, we combine the 3D-RISM theory with a structure optimization method (the Quasi-Newton method), and optimize the telomere structure in aqueous solution of electrolytes to investigate the stability of these structures.

II. COMPUTATIONAL METHOD

The energy function that we used in the present work is given by the sum of two terms: the conformational energy F_{conf} of the telomeric DNA molecule itself and the solvation free energy $\Delta\mu$ for the interaction of the telomeric DNA with the surrounding solvent:

$$F_{tot} = E_{conf} + \Delta\mu \tag{1}$$

The conformational energy E_{conf} consists of bonding, bending, torsion-energy, Lennard-Jones, and electrostatic terms. Note that solvation effects were accounted for not by the solvation energy, but by the solvation free energy, because we wanted to estimate the relative energies and the force from solvation of each solute configuration.

The solvation free energy is calculated by 3D-RISM theory. The detailed formulation of the 3D-RISM theory is provided in ref 38. Here, only a brief interpretation of the theory is provided to help some readers to understand the "physical" aspect of the theory.

Let us consider the average density of solvent molecules at a position around a telomeric DNA molecule. When the position is far from the telomeric DNA molecule so as to be regarded as the bulk, the density will be constant, which is the same as in the pure liquid. On the other hand, when it is near telomeric DNA, the density will be "perturbed" significantly by the field due to the telomeric DNA and be different from that in the bulk, depending on the strength of the perturbation. The 3D-RISM theory can be interpreted as a "nonlinear" perturbation theory as follows.

Let us denote the constant density of solvent atom γ at the bulk, the density nearby telomeric DNA, and the density response to the perturbation as ρ, $\rho_\gamma(\mathbf{r})$, and $\Delta\rho_\gamma(\mathbf{r})$, respectively. Then, the statement above can be expressed as

$$\rho_\gamma(\mathbf{r}) = \rho + \Delta\rho_\gamma(\mathbf{r}) \tag{2}$$

The density response to the perturbation can be expressed on the basis of the 3D-RISM theory as

$$\Delta\rho_\gamma(\mathbf{r}) = \sum_\alpha \int \chi_{\gamma\alpha}(\mathbf{r},\mathbf{r}')\rho_\gamma c_\alpha(\mathbf{r}')\, d\mathbf{r}' \tag{3}$$

where the $c_\alpha(\mathbf{r}')$ is the "re-normalized" perturbation due to the telomeric DNA, to which several approximate equations have been devised: for example, the Kovalenko−Hirata (KH) approximation[47,48] takes the following expression,

$$h_\gamma^{uv}(\mathbf{r}) = \begin{cases} \exp(\chi) - 1 & \text{for} \quad \chi \le 0 \\ \chi & \text{for} \quad \chi > 0 \end{cases}$$

$$\chi = -\beta u_\gamma^{uv}(\mathbf{r}) + h_\gamma^{uv}(\mathbf{r}) - c_\gamma^{uv}(\mathbf{r}) \tag{4}$$

In the expression, $u_\gamma(\mathbf{r})$ is the direct interaction potential exerted on water molecules from telomeric DNA, $\beta = 1/(k_B T)$, and $h_\gamma(\mathbf{r})$ is the density fluctuation of solvation at position $\mathbf{r}$, normalized by the bulk density, namely,

$$h_\gamma(\mathbf{r}) = \Delta\rho_\gamma(\mathbf{r})/\rho \tag{5}$$

The three-dimensional distribution function used in this study is defined from $h_\gamma(\mathbf{r})$ by

$$g_\gamma(\mathbf{r}) = h_\gamma(\mathbf{r}) + 1 \tag{6}$$

It is not only the direct interaction $u(\mathbf{r})$ with DNA that perturbs the density of solvent at a certain position but also that from solvent molecules at the other positions, whose density is also perturbed by the existence of the same DNA. Such "indirect" perturbations are renormalized into the terms including $(h_\gamma(\mathbf{r}) - c_\gamma(\mathbf{r}))$. Such renormalization makes the perturbation highly "nonlinear."

The response function $\chi_{\alpha\gamma}(\mathbf{r},\mathbf{r}')$ is equivalent to the density pair correlation function of pure (bulk) solvent,

$$\rho^2\chi_{\alpha\gamma}(\mathbf{r},\mathbf{r}') = \langle\delta\rho_\alpha^{(0)}(\mathbf{r})\delta\rho_\gamma^{(0)}(\mathbf{r}')\rangle \quad (7)$$

where $\delta_\alpha^{(0)}(\mathbf{r})$ is the density fluctuation of atom σ in the pure liquid defined by $\delta\rho_\alpha^{(0)}(\mathbf{r}) = \rho_\alpha^{(0)}(\mathbf{r}) - \rho_\alpha$. This response function can be obtained in advance from the one-dimensional RISM theory.

It is a straightforward task to obtain the one-dimensional distribution, or the radial distribution function (RDF), from the 3D-distribution function. The RDFs between position $\mathbf{r}_x$ and solvent γ can be obtained by averaging the 3D-distribution function over the direction around a specified center:

$$g_{x\gamma}(r) = \frac{1}{4\pi}\int g(\mathbf{r}_x + \mathbf{r})\, d\hat{\mathbf{r}} \quad (8)$$

where $\hat{\mathbf{r}}$ is a direction of vector $\mathbf{r}$, and $\mathbf{r}_x$ indicates a center for the averaging.

We consider aqueous solution of electrolytes for the solvent and a DNA for the solute. The solvation free energy (SFE) $\Delta\mu$ is calculated by using the 3D extension of the Singer−Chandler formula,[49,50]

$$\Delta\mu = \rho k_B T \sum_\alpha \int_{V_{cell}} d\mathbf{r}\left[\frac{1}{2}(h_\gamma(\mathbf{r}))^2\Theta(-h_\gamma(\mathbf{r})) - c_\gamma(\mathbf{r}) - \frac{1}{2}h_\gamma(\mathbf{r})\, c_\gamma(\mathbf{r})\right] \quad (9)$$

For the pair potentials between interaction sites of every species, we employ the common model which consists of the Lennard-Jones (LJ) and electrostatic interaction terms

$$u_{\alpha\gamma}(r) = 4\varepsilon_{\alpha\gamma}\left[\left(\frac{\sigma_{\alpha\gamma}}{r}\right)^{12} - \left(\frac{\sigma_{\alpha\gamma}}{r}\right)^{6}\right] + \frac{1}{4\pi\varepsilon_0}\frac{q_\alpha q_\gamma}{r} \quad (10)$$

where $\varepsilon_{\alpha\gamma}$ and $\sigma_{\alpha\gamma}$ are the LJ energy and size parameters for a pair of solute site α and solvent site γ, respectively, ε_0 is a dielectric constant of vacuum, and q_α is the partial charge on site α.

To evaluate the optimized structure in solutions, we have to calculate the gradients of solvation free energy with respect to the atomic coordinate of the solute molecule on the basis of the 3D-RISM theory. The analytical expression of the free energy gradient was presented by Sato et al. in the framework of RISM-SCF/MCSCF theory[51] and the expression is easily extented to the 3D-RISM formalism.[52,53] For the 3D-RISM/KH theory, it is expressed as

$$\frac{\partial\Delta\mu}{\partial\mathbf{R}_a} = \sum_\gamma \rho_\gamma \int d\mathbf{r}\frac{\partial u_\gamma^{uv}(\mathbf{r})}{\partial\mathbf{R}_a} g_\gamma^{uv}(\mathbf{r}) \quad (11)$$

where $\mathbf{R}_a$ and $u_\gamma^{uv}(\mathbf{r})$ represent the position vector of solute site a and the interaction potential energy, respectively. The gradient of total free energy of the DNA in solution, eq 1, can be written as

$$\frac{\partial F_{tot}}{\partial\mathbf{R}_a} = \frac{\partial E_{conf}}{\partial\mathbf{R}_a} + \sum_\gamma \rho_\gamma \int d\mathbf{r}\frac{\partial u_\gamma^{uv}(\mathbf{r})}{\partial\mathbf{R}_a} g_\gamma^{uv}(\mathbf{r}) \quad (12)$$

where the first term of the right-hand side of the equation is calculated analytically. We performed the optimization of DNA structure to minimize the total free energy F_{tot} by using the quasi-Newton method with eq 12.

The purpose of the paper is to clarify the structural stability of human telomere in molecular detail, not to reproduce the experimental results quantitatively. Therefore, we used the potential parameters that have been employed commonly in our previous studies and have reproduced experimental results reasonably well.[39−42,46,54−57] For telomeric DNA and ions, we employ the parameters from the Amber-02 force field, which contains bonding, bending, torsional, van der Waals and electrostatic energies.[58] The conformational energy was calculated by the standard molecular mechanics method. The fragment of human telomere DNA with d[AGGG(TTAGGG)$_3$] sequence was prepared as the solute. For the basket-, propeller-, and hybrid-type conformations, the initial coordinates were taken from the Protein Data Bank listed in Table 2, and the cation and the water molecule were removed from PDB structures and then hydrogen atoms were added at proper positions. For the chair-type conformation (which no PDB data is available), we modeled the structure by modifying the loop bases and backbone of hybrid-type structure. Illustrative views of the structures are exhibited in Figure 1. We use the SPC/E model[59] with the hydrogen Lennard-Jones term (σ = 1.0 Å and ε = 0.046 kcal/mol) for the water atoms.[60] The LJ parameter between unlike atomic sites is determined from the standard Lorentz−Berthelot combination rules. All calculations are carried out for ambient water at temperature T = 298.15 K. The 3D-RISM/KH equations were solved on a grid of 256^3 points in a cubic cell of

Table 2. Protein Data Bank ID for Each Structure

	PDB ID
basket	143D
propeller	1KF1
hybrid	2E4I

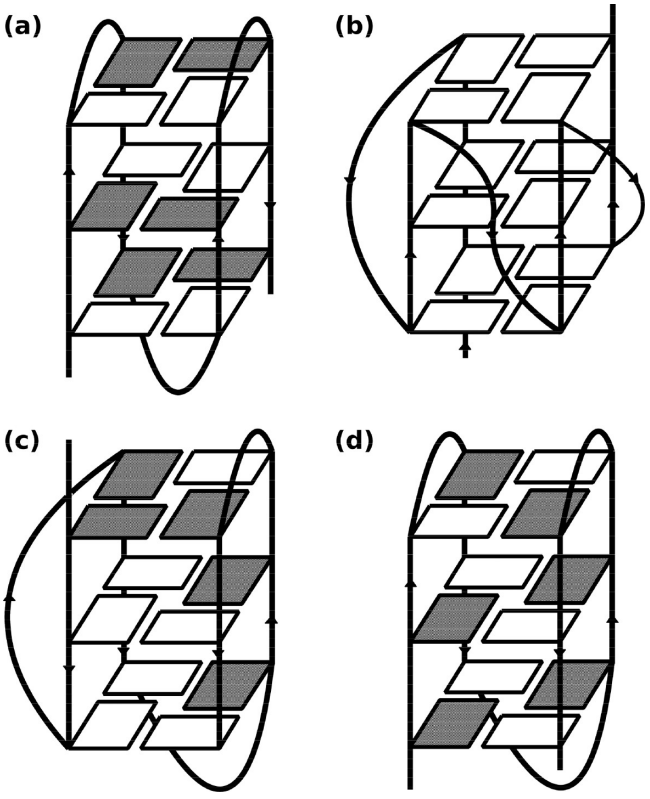

Figure 1. Schematic structure of (a) basket-, (b) propeller-, (c) hybrid-, and (d) chair-type. The gray and white boxes represent guanine bases in syn and anti conformations, respectively.

size 64 Å^3. The grid space of 0.25 Å is fine enough to obtain the results without significant numerical errors The grid space of 0.25 is fine enough to obtain the results without significant numerical errors: the errors estimated for the solvation free energy of chair-type structure in water upon changing the grid width from 0.25 to 0.5 is less than 0.001%. To converge the equations, we used the modified direct inversion in the iterative subspace (MDIIS) method.[61]

The root-mean-square displacement (rmsd) without hydrogen atoms between the structures of minimum F_{tot} and of the starting PDB for the four structures studied are 1.95 (basket), 1.44 (propeller), 1.99 (hybrid), and 2.91 (chair) in water; 1.95 (basket), 1.40 (propeller), 2.01 (hybrid), and 2.93 (chair) in NaCl solutions; 1.89 (basket), 1.37 (propeller), 1.99 (hybrid), and 2.91 (chair) in KCl solutions.

III. RESULTS AND DISCUSSION

Pure Water. *Free Energies.* The free energies (F_{tot}) for the optimized structure of the each G-quadruplex DNA in pure water are tabulated in Table 3, along with the contributions from the conformational energy (E_{conf}) and those from the solvation free energies due to solvent ($\Delta\mu_{water}$). The telomeric DNA conformations were optimized in pure water on the basis of the method described in the previous section.

Table 3. Total Energy F_{tot} and Its Components (Conformation Energy E_{conf} and Solvation Free Energy $\Delta\mu$) of Each Structure in Water[a]

	F_{tot}	E_{conf}	$\Delta\mu$
basket	−4098.0	1886.5	−5984.5
propeller	−4070.6	1381.6	−5452.2
hybrid	−4085.0	1591.2	−5676.2
chair	−4111.1	1675.1	−5786.2

[a] Energy unit is kcal/mol.

The result indicates that the conformational stability is largely dominated by the hydration free energy. The most stable structure among the four quadruplexes in water is the chair-type structure, which is followed by basket-, hybrid-, and propeller-type structures in that order. The result for E_{conf} suggests that the propeller structure is the most stable one in the environment where there is no water, and that the basket-type is the least stable structure in that condition. The result for the propeller-type structure does make sense because it is found in a crystal state that is in low moisture condition. (Although we compared the stabilities among the four models of G-quadruplex, it does not necessarily mean that a telomere actually takes the chair-form, because a telemere in pure water is known to take more or less random coil-like structures. We calculated the free energy of the quadruplex in pure water to get insight into how significant the effect of hydration upon the quadruplex structures is.)

Solvation Structure. The distribution functions $g(\mathbf{r})$ of water oxygen around the G-quadruplex DNA in pure water are depicted with iso-surface plots in Figure 2 for the (a) basket-, (b) propeller- and (c) hybrid- (d) chair-forms of the DNA with d[AGGG(TTAGGG)$_3$] sequence. The distribution functions are those normalized by the bulk solvent density, that is, $g(\mathbf{r}) = 1$ at bulk. The threshold value for the iso-surface plots is set at 3.0 for water, meaning that only $g(\mathbf{r})$ having values greater than 3.0 is depicted. This is just for the purpose of presentation, and the

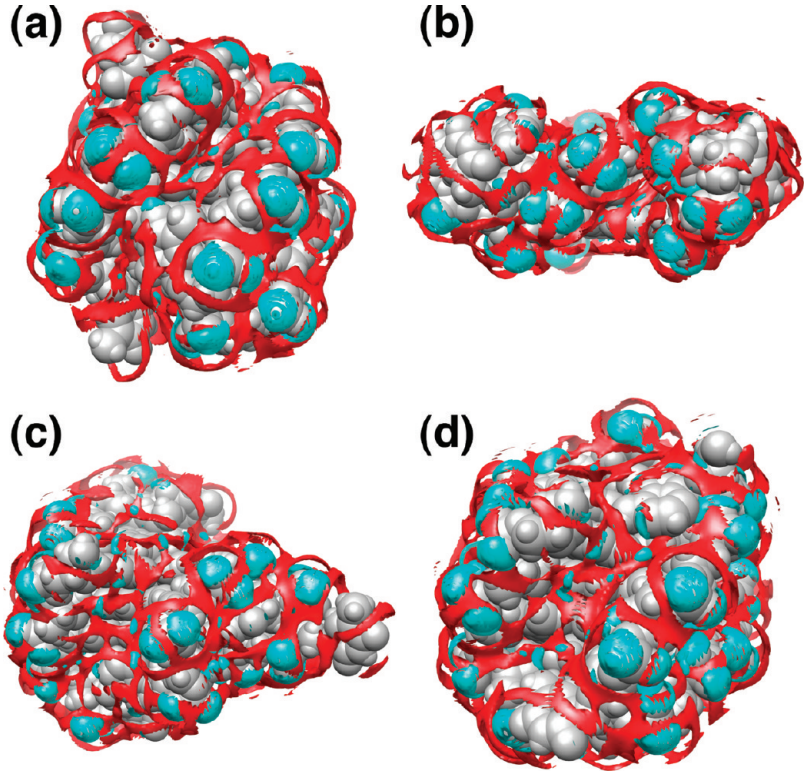

Figure 2. Optimized structures of telomeric DNA and the distributions of water oxygen (red) and hydrogen (cyan) of (a) basket-, (b) propeller-, (c) hybrid-, and (d) chair-type structures. The respective density thresholds were 3.0.

dx.doi.org/10.1021/jp1096019 |J. Phys. Chem. B 2011, 115, 2408–2416

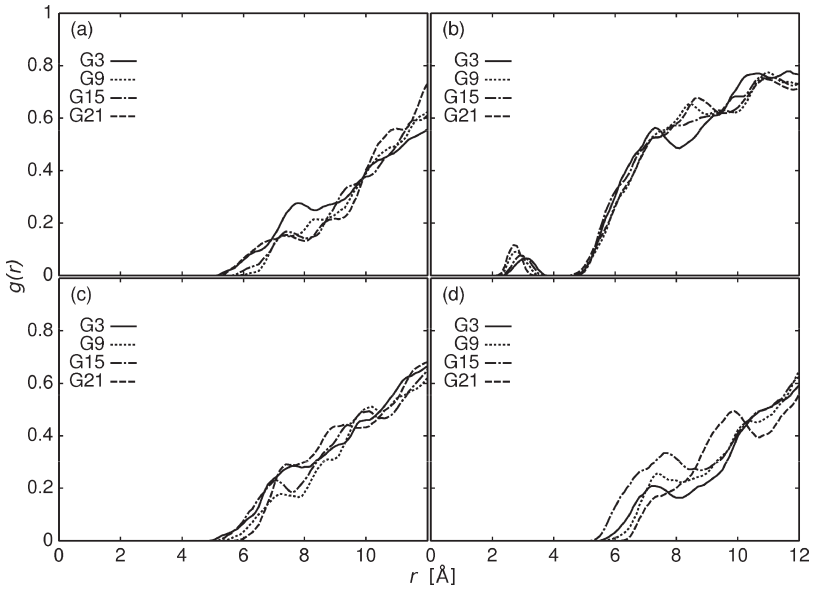

Figure 3. RDFs between water oxygen and oxygens on the middle layer guanines of (a) basket-, (b) propeller-, (c) hybrid-, and (d) chair-type structures in water.

following arguments are unchanged with the choice of the threshold value employed to draw the figures.

The features of hydration structure for telomeric DNA is essentially the same as that for the canonical double helix of DNA, obtained in our earlier study in which we have compared the hydration structure obtained from the 3D-RISM theory with that from the molecular dynamics simulation.[45] The phosphate groups are covered with a cyan surface, indicating that the group is solvated primarily by hydrogen atoms of water. Of course, oxygen atoms associated with the hydrogen atoms are distributed near the hydrogen atoms, but they are less distinct due to the thermal fluctuation so that it is not discernible with the present threshold value of $g(\mathbf{r})$. In contrast to the phosphate groups, the spaces between the groups are filled by a red surface, indicating that the region is solvated primarily with oxygen atoms of water. The oxygen distribution is forming a characteristic network (or train) pattern. There will not be any doubt that such hydration is the dominant factor to stabilize the telomere structure, since the structures just collapse if one tries to optimize it in vacuum.

Depicted in Figure 3 is the radial distribution function (RDF) of water oxygen around the oxygen atoms in the middle layer guanines of each conformation: The place is known to be cavities where cations are bound in the electrolyte solutions. The RDFs indicate that there is no water molecule bound in that cavity.

Aqueous Solutions of Sodium Chloride. *Free Energies.* The free energies for the each structure of telomeric DNA in 0.1 M NaCl solutions are tabulated in Table 4, including F_{tot} and the contributions from the conformational energy (E_{conf}) and those from the solvation free energies ($\Delta\mu$) due to solvent ($\Delta\mu_{water}$) and salts ($\Delta\mu_{electrolyte}$). The increasing order of the free energy and each contribution are as follows: F_{tot}, basket < chair < hybrid < propeller; $\Delta\mu$, basket < chair < hybrid < propeller; $\Delta\mu_{water}$, basket < chair < hybrid < propeller; $\Delta\mu_{electrolyte}$, basket < chair < hybrid < propeller; E_{conf}, propeller < hybrid < chair < basket.

The results for the total free energy show a different order from the case in pure water: the basket-type is the most stable, while the chair-type is the second. So, the results indicate undoubtedly that the electrolyte gives significant effects on the telomere structure. The differences in the free energies between the first and second stable structures are about 26.7 kcal/mol (or ~1.2 kcal/mol-base), which is even much larger than the corresponding number concerning the B−Z transition of DNA, which is ~0.3 kcal/mol of base.[46] The result is in qualitative accord with the experimental result due to the NMR spectroscopy, which has identified the basket-type structure in the solution.[17]

Table 4. Total Energy F_{tot} and Its Components (Conformation Energy E_{conf} and Solvation Free Energy $\Delta\mu$) of Each Structure in NaCl 0.1 M Solution[a]

	F_{tot}	E_{conf}	$\Delta\mu$	$\Delta\mu_{water}$	$\Delta\mu_{electrolyte}$
basket	−4294.1	1886.6	−6180.7	−2163.7	−4017.0
propeller	−4257.6	1396.1	−5653.7	−1820.2	−3833.5
hybrid	−4261.8	1652.0	−5913.8	−1965.7	−3948.1
chair	−4267.4	1672.7	−5940.1	−1979.8	−3960.3

[a] $\Delta\mu_{water}$ and $\Delta\mu_{electrolyte}$ are the contributions of solvation free energy from water and salts, respectively. Energy unit is kcal/mol.

As long as the conformational energy is concerned, the propeller-type, the structure found in the crystal, is the lowest. However, the solvation free energy of this structure is rather high, which makes the overall stability lower compared to the other structures. The results suggest that telomeric DNA undergoes a significant structural change upon crystallization from solutions.

It may be worthwhile to mention about the numerical accuracy of our results, because two of the reviewers asked the same question, "what is the error bar on the total energy?" The question is reasonable in a sense, because the difference in the free energy between the most and second stable structures of the quadruplex in NaCl solutions, for example, is about 27 kcal/mol or ~0.5% of the total free energy, which is easily within an error bar in an ordinary experiment or a simulation. However, such numbers are typical in the free energy difference between two conformations of DNA as is stated above.[46] So, any successful method, either experimental or theoretical, should attain such

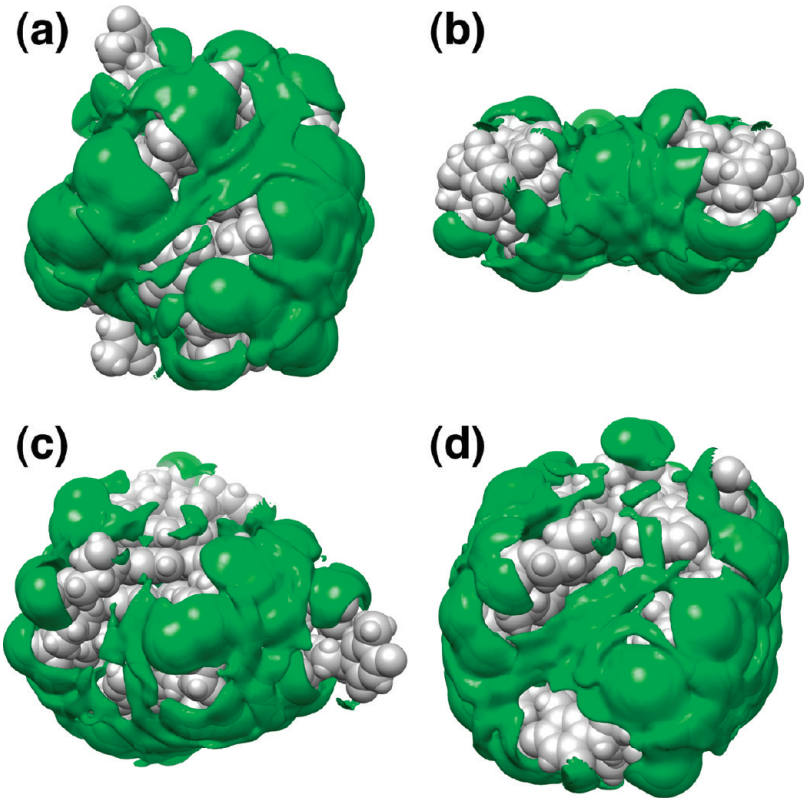

Figure 4. Optimized structures of telomeric DNA and the distributions of sodium (green) of (a) basket-, (b) propeller-, (c) hybrid-, and (d) chair-type structures. The respective density threshold is 12.0.

accuracy to characterize the difference in the stability of DNA structures. It will be extremely challenging for a molecular simulation due to slow convergence in statistics to calculate the free energy or the probability distribution of the structures. In the sharp contrast, our method is free from "error bars", because our theory is essentially an analytical theory in which an averaging over the configurations including both the telomere and water is made analytically by means of the statistical mechanics. So, the results are completely accurate within the approximation involved in the theory.

Distribution of Electrolytes. The distribution of the electrolytes (Na^+ and Cl^-) in 0.1 M solutions around telomeric DNA is shown in Figure 4. The phosphate groups are covered by a green surface, indicating that the groups are primarily solvated with Na^+ ions in the electrolyte solution. We notice that the distribution of Cl^- ions disappears at the threshold value 12.0 because the net charge of telomeric DNA is negative: the repulsive force between charges with the same sign is strong at low concentration. The picture suggests that Na^+ ions are bound directly in contact with phosphate oxygen, not indirectly with intermediate water molecules in between the phosphate and the ion. The picture also suggests that the affinity of Na^+ ions to the bases are not so large.

Shown in Figure 5 is the Na^+ iso-surface, in which the threshold value is set at 30.0, to investigate ions distribution on the binding sites in telomeric DNA. A distinct pair of peaks is seen in the distribution for all the four structures of G-quadruplex, which indicate the existence of Na^+ ions bound to the telomeric DNA. The high threshold value (>30.0) tells us how strong the binding affinity is. Such a characteristic double peak has been observed also by the X-ray diffraction study.[18]

Aqueous Solutions of Potassium Chloride. *Free Energies.* The free energies (F_{tot}) of the four structures of the telomere G-quadruplex in potassium chloride solutions are tabulated in Table 5, along with the contributions from the conformational energy (E_{conf}) and those from the solvation free energies ($\Delta\mu$) due to solvent ($\Delta\mu_{water}$) and salts ($\Delta\mu_{electrolyte}$). The increasing order of the free energy and each contribution are as follows: F_{tot}, chair < basket < hybrid < propeller; $\Delta\mu$, basket < chair < hybrid < propeller; $\Delta\mu_{water}$, basket < chair < hybrid < propeller; $\Delta\mu_{electrolyte}$, basket < chair < hybrid < propeller; E_{conf}, propeller < hybrid < chair < basket. Apparently, the order of the stability coincides with that in pure water, and it is reversed from the NaCl solution between the basket-type and chair-type conformations. The results suggest that the effect of the potassium ion upon the structure is not so strong as the sodium ion to change the order of the stability determined in pure water.

Distribution of Electrolytes. Shown in Figure 6 is the K^+ iso-surface (purple spots), in which the threshold value is set at 30.0 as in the case of Na^+. Distinct from the case of sodium ions, the two spots of distributions are observed only in the three conformations: chair-, basket-, and propeller-type conformations. Nothing is found in the hybrid-type conformation. The results suggest that the affinity of potassium ions to the cavity is less than that of the sodium ions. To verify this, we plotted RDF of Na^+ and K^+ ions around the oxygen atom in the middle layer guanines of each conformation in Figure 7. The figure clearly indicates that the affinity of K^+ to the binding site is weaker than that of Na^+. The finding is consistent with the free energy results which indicate that the effect of K^+ on the structure of telomere is weaker than that of Na^+.

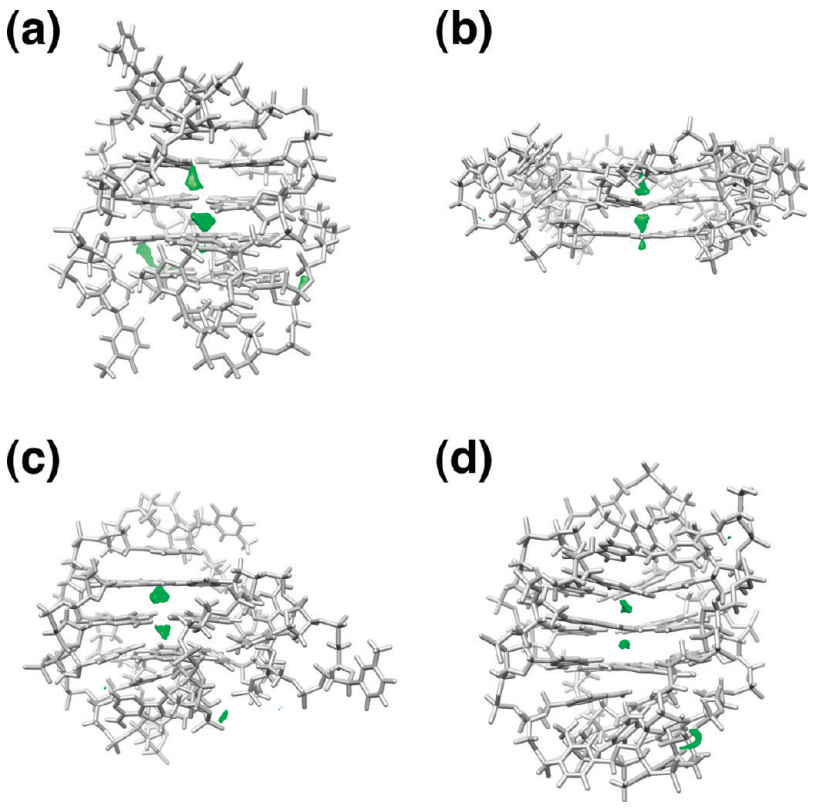

Figure 5. Distributions of sodium (green) around (a) basket-, (b) propeller-, (c) hybrid-, and (d) chair-type structures. Telomere structures are depicted by stick for the sake of visualization. The respective density threshold is 30.0.

Table 5. Total Energy F_{tot} and Its Components (Conformation Energy E_{conf} and Solvation Free Energy $\Delta\mu$) of Each Structure in KCl 0.1 M Solution[a]

	F_{tot}	E_{conf}	$\Delta\mu$	$\Delta\mu_{water}$	$\Delta\mu_{electrolyte}$
basket	−4284.3	1849.7	−6133.0	−2211.0	−3923.0
propeller	−4251.4	1369.0	−5620.4	−1879.5	−3740.9
hybrid	−4271.6	1591.4	−5863.0	−2003.8	−3859.2
chair	−4299.7	1675.1	−5974.8	−2074.7	−3900.1

[a] $\Delta\mu_{water}$ and $\Delta\mu_{electrolyte}$ are the contributions of solvation free energy from water and salts, respectively. Energy unit is kcal/mol.

IV. CONCLUDING REMARKS

The free energy and the solvation sturctures of the G-quadruplex telomeric DNA in pure water and in the 0.1 M aqueous solutions of sodium and potassium chlorides were calculated on the basis of the 3D-RISM theory. To find the most stable structure of each G-quadruplex in the aqueous solutions, the free energy is minimized in the solutions on the basis of the quasi-Newton method using the analytical derivative of the solvation free energy obtained from 3D-RISM.

In pure water, the chair-type conformation was found to be the most stable structure, which is followed by basket-, hybrid-, and propeller-type structures in that order. It was clarified that the order of the stability is determined essentially by the solvation free energy, not by the conformational energy.

The order of the conformational stability of the G-quadruplex in 0.1 M NaCl solutions is different from that in pure water. The basket-type structure becomes the most stable one in the electrolyte solution. The theoretical finding is consistent with the experimental observation due to NMR. The energy component analysis clearly shows that the contribution from the electrolytes dominates the free energy change. We also found a distinct pair of peaks in the distribution of sodium ions, at the spaces between the G-quartets stacked in the telomeric DNA. The distinct pattern of the ion distributions in telomeric DNA is in complete accord with the experimental observations. The reversed order of the conformational stability was attributed to the salt effect, especially, to that from the Na^+ ions bound at interstrand spaces of DNA.

Our results for the conformational stability in KCl solutions predict that the order of stability is not changed from that in pure water; that is, the chair-type is the most stable one, although no experimental data are available at the moment to be compared with. The finding suggests that the effect of the potassium ion upon the structure is not so strong as the sodium ion to change the order of the stability determined in pure water. The result is consistent with our finding for RDFs of the ions bound at the interstrand spaces in DNA, which indicates clearly that the affinity of K^+ to the binding site is weaker than that of Na^+.

Concerning the structural stability of the telomere in NaCl and KCl solutions, one of the reviewers brought a very interesting experimental result to our attention. Hud and co-workers performed a titration experiment of NaCl by KCl solutions and found that K^+ ions replace Na^+ ions in the biding site of telomere quadruplex in the titration process.[63] The experimental setup is not entirely the same as the one on which we have made the theoretical analysis. They used a telomere dimer $[d(G3T4G3)]_2$, not a single chain human telomere

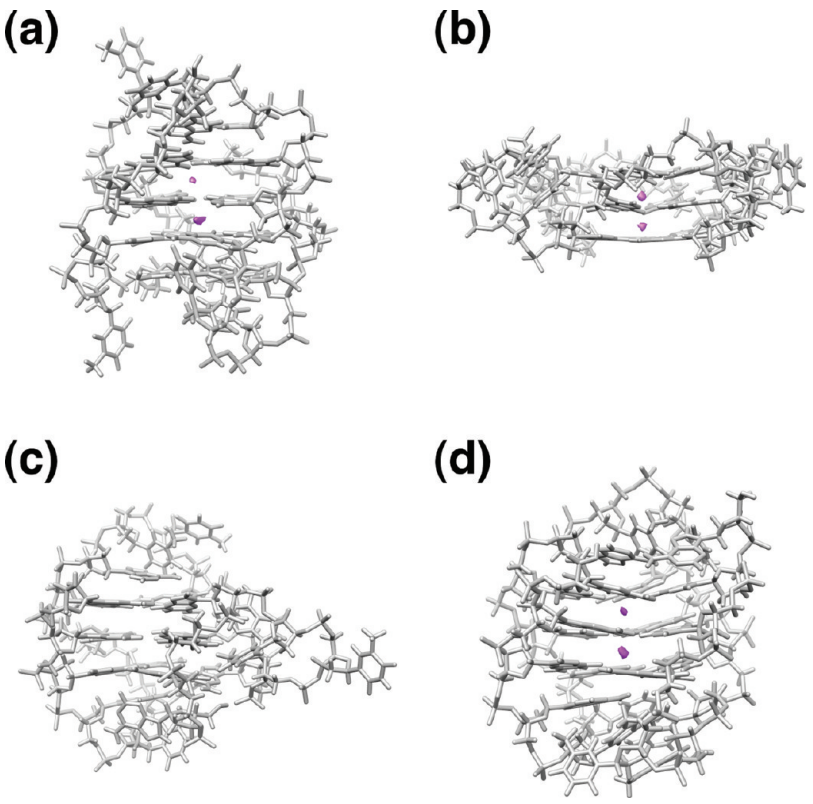

Figure 6. Distributions of potassium (purple) around (a) basket-, (b) propeller-, (c) hybrid-, and (d) chair-type structures. Telomere structures are depicted by stick for the sake of visualization. The respective density threshold is 30.0.

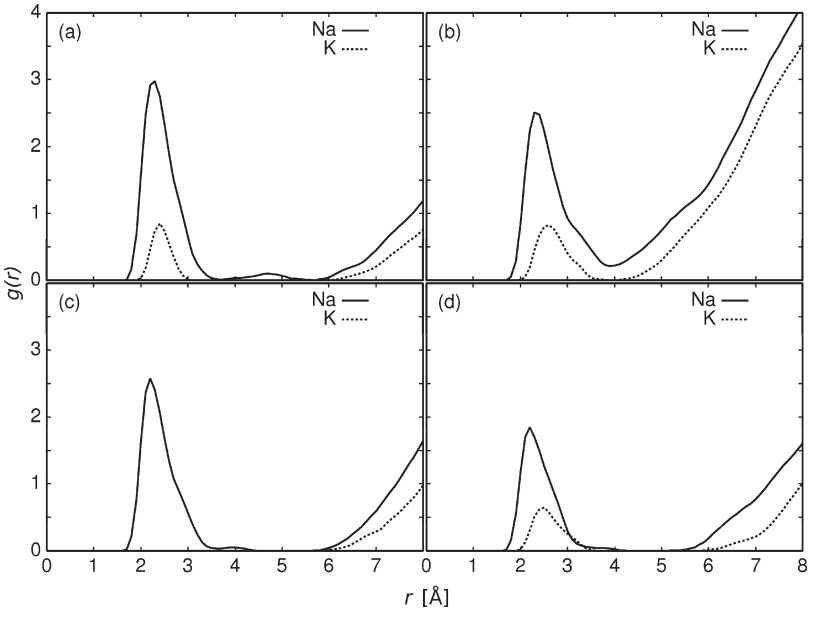

Figure 7. RDFs between ion and oxygens on the middle layer guanines of (a) basket-, (b) propeller-, (c) hybrid-, and (d) chair-type structures in water. The solid line indicates sodium ion, and the dot line is potassium ion.

d(AG3(T2AG3)3). Therefore, the folded telomere structures and numbers of binding cations between the theory and experiment cannot be the same. Nevertheless, our theoretical results are apparently consistent with the experimental results. According to our calculation, the total free energy of basket-type in 0.1 M NaCl solution is −4294.1 kcal/mol, whereas that of chair-type in 0.1 M KCl solution is −4299.7 kcal/mol. The result indicates that the chair-type in KCl solutions is more stable than the basket-type in NaCl solutions. This result implies that Na^+ may be replaced by K^+ in the titration experiment as in the results by Hub. We thank the referee for bringing the paper to our attention.

■ ACKNOWLEDGMENT

We thank Prof. Matsumoto, Dr. Tanoue, Mr. Ohgidani, and Mr. Takeda in Sojo University and Prof. Yoshida in IMS for fruitful discussions. This work is supported by the grant from Grand Challenges in Next-Generation Supercomputing Project, Nanoscience Program, and the Grant-in Aid for Scientific Research on Innovative Areas "Molecular Science of Fluctuations toward Biological Functions" from the MEXT in Japan. Molecular graphics images were produced using the UCSF Chimera package.[62]

■ REFERENCES

(1) Harley, C. B.; Futcher, A. B.; Greider, C. W. *Nature* **1990**, *345*, 458.
(2) Zahler, A. M.; Williamson, J. R.; Cech, T. R.; Prescott, D. M. *Nature* **1991**, *350*, 718.
(3) Burge, S.; Parkinson, G. N.; Hazel, P.; Todd, A. K.; Neidle, S. *Nucleic Acids Res.* **2006**, *34*, 5402.
(4) Mergny, J. L.; Hélène, C. *Nat. Med.* **1998**, *4*, 1366.
(5) Kerwin, S. M. *Curr. Pharm. Des.* **2000**, *6*, 441.
(6) Perry, P. J.; Jenkins, T. C. *Mini-Rev. Med. Chem.* **2001**, *1*, 31.
(7) Neidle, S.; Parkinson, G. *Nat. Rev. Drug. Des.* **2002**, *1*, 383.
(8) Hurley, L. H. *Nat. Rev. Cancer* **2002**, *2*, 188.
(9) Riou, J. F. *Curr. Med. Chem. Anti-Cancer Agents* **2004**, *4*, 439.
(10) Jing, N.; Sha, W.; Li, Y.; Xiong, W.; Tweardy, D. J. *Curr. Pharm. Des.* **2005**, *11*, 2841.
(11) Phan, A. T.; Kuryavyi, V.; Gaw, H. Y.; Patel, D. J. *Nat. Chem. Biol.* **2005**, *1*, 167.
(12) Doherty, K. M.; Sharma, S.; Gupta, R.; Brosh, R. M., Jr. *Recent Pat. Anti-cancer Drug Discovery* **2006**, *1*, 185.
(13) Oganesian, L.; Bryan, T. M. *Bioessays* **2007**, *29*, 155.
(14) Neidle, S. *FEBS J.* **2010**, *277*, 1118.
(15) Burge, S.; Parkinson, G. N.; Hazel, P; Todd, A. K.; Neidle, S. *Nucleic Acids Res.* **2006**, *34*, 5402.
(16) Chaires, J. B. *FEBS J.* **2010**, *277*, 1098.
(17) Wang, Y.; Patel, D. J. *Structure* **1993**, *1*, 263.
(18) Parkinson, G. N.; Lee, M. P. H.; Neidle, S. *Nature* **2002**, *417*, 876.
(19) Ambrus, A.; Chen, D.; Dai, J. X.; Bialis, T.; Jones, R. A.; Yang, D. Z. *Nucleic Acids Res.* **2006**, *34*, 2723.
(20) Luu, K. N.; Phan, A. T.; Kuryavyi, V.; Lacroix, L.; Patel, D. J. *J. Am. Chem. Soc.* **2006**, *128*, 9963.
(21) Phan, A. T.; Luu, K. N.; Patel, D. J. *Nucleic Acids Res.* **2006**, *34*, 5715.
(22) Phan, A. T.; Kuryavyi, V.; Luu, K. N.; Patel, D. J. *Nucleic Acids Res.* **2007**, *35*, 6517.
(23) Dai, J.; Punchihewa, C.; Ambrus, A.; Chen, D.; Jones, R. A.; Yang, D. *Nucleic Acids Res.* **2007**, *35*, 2440.
(24) Dai, J.; Carver, M.; Punchihewa, C.; Jones, R. A.; Yang, D. *Nucleic Acids Res.* **2007**, *35*, 4927.
(25) Xu, Y.; Noguchi, Y.; Sugiyama, H. *Bioorg. Med. Chem.* **2006**, *14*, 5584.
(26) Matsugami, A.; Xu, Y.; Noguchi, Y.; Sugiyama, H.; Katahira, M. *FEBS J.* **2007**, *274*, 3545.
(27) Okamoto, K.; Sannohe, Y.; Mashimo, T.; Sugiyama, H.; Terazima, M. *Bioorg. Med. Chem.* **2008**, *16*, 6873.
(28) Sannohe, Y.; Sato, K.; Matsugami, A.; Shinohara, K.; Mashimo, T.; Katahira, M.; Sugiyama, H. *Bioorg. Med. Chem.* **2009**, *17*, 1870.
(29) He, Y. J.; Neumann, R. D.; Panyutin, I. G. *Nucleic Acids Res.* **2004**, *32*, 5359.
(30) Su, D. G. T.; Fang, H. F.; Gross, M. L.; Taylor, J. S. A. *Proc. of the Natl. Acad. Sci. U. S. A.* **2009**, *106*, 12861.
(31) Redon, S.; Bombard, S.; Elizondo-Riojas, M. A.; Chottard, J. C. *Nucleic Acids Res.* **2003**, *31*, 1605.
(32) Chowdhury, S.; Bansal, M. *J. Phys. Chem. B* **2001**, *105*, 7572.
(33) Gavathiotis, E.; Searle, M. S. *Org. Biomol. Chem.* **2003**, *1*, 1650.
(34) Gavathiotis, E.; Heald, R. A.; Stevens, M. F. G.; Searle, M. S. *J. Mol. Biol.* **2003**, *334*, 25.
(35) Hazel, P.; Huppert, J.; Balasubramanian, S.; Neidle, S. *J. Am. Chem. Soc.* **2004**, *126*, 16405.
(36) Agrawal, S.; Ojha, R. P.; Maiti, S. *J. Phys. Chem. B* **2008**, *112*, 6828.
(37) Taylor, A.; Taylor, J.; Watson, G. W.; Boyd, R. J. *J. Phys. Chem. B* **2010**, *114*, 9833.
(38) Hirata, F., Ed. *Molecular Theory of Solvation*; Kluwer: Dordrecht, The Netherlands, 2003.
(39) Imai, T.; Hiraoka, R.; Kovalenko, A.; Hirata, F. *J. Am. Chem. Soc.* **2005**, *127*, 15334.
(40) Imai, T.; Hiraoka, R.; Kovalenko, A.; Hirata, F. *Proteins* **2007**, *66*, 804–813.
(41) Yoshida, N.; Phongphanphanee, S.; Maruyama, Y.; Imai, T.; Hirata, F. *J. Am. Chem. Soc.* **2006**, *128*, 12042.
(42) Yoshida, N.; Phongphanphanee, S.; Hirata, F. *J. Phys. Chem. B* **2007**, *111*, 4588.
(43) Ikuta, Y.; Maruyama, Y.; Matsugami, M.; Hirata, F. *Chem. Phys. Lett.* **2007**, *433*, 403.
(44) Maruyama, Y.; Matsugami, M.; Ikuta, Y. *Phys. Rev. B: Condens. Mater. Phys.* **2007**, *10*, 315.
(45) Yonetani, Y.; Maruyama, Y.; Hirata, F.; Kono, H. *J. Chem. Phys.* **2008**, *128*, 185102.
(46) Maruyama, Y.; Yoshida, N.; Hirata, F. *J. Phys. Chem. B* **2010**, *114*, 6464.
(47) Kovalenko, A.; Hirata, F. *J. Phys. Chem. B* **1999**, *103*, 7942.
(48) Kovalenko, A.; Hirata, F. *J. Chem. Phys.* **2000**, *112*, 10391.
(49) Singer, S. J.; Chandler, D. *Mol. Phys.* **1985**, *55*, 621.
(50) Kovalenko, A.; Hirata, F. *J. Chem. Phys.* **1999**, *110*, 10095.
(51) Sato, H.; Hirata, F.; Kato, S. *J. Chem. Phys.* **1996**, *105*, 1546.
(52) Yoshida, N.; Hirata, F. *J. Comput. Chem.* **2006**, *27*, 453.
(53) Gusarov, S.; Ziegler, T.; Kovalenko, A. *J. Phys. Chem. A* **2006**, *110*, 6083.
(54) Imai, T.; Harano, Y.; Kinoshita, M.; Kovalenko, A.; Hirata, F. *J. Chem. Phys.* **2006**, *125*, 024911.
(55) Phongphanphanee, S.; Yoshida, N.; Hirata, F. *Chem. Phys. Lett.* **2007**, *449*, 433.
(56) Phongphanphanee, S.; Yoshida, N.; Hirata, F. *J. Am. Chem. Soc.* **2008**, *130*, 1540.
(57) Phongphanphanee, S.; Yoshida, N.; Hirata, F. *J. Mol. Liq.* **2009**, *147*, 107.
(58) Cieplak, P.; Caldwell, J.; Kollman, P. *J. Comput. Chem.* **2001**, *22*, 1048.
(59) Berendsen, H. J. C.; Grigera, J. R.; Straatsma, T. P. *J. Chem. Phys.* **1987**, *91*, 6269.
(60) Pettitt, B. M.; Rossky, P. J. *J. Chem. Phys.* **1982**, *77*, 1451.
(61) Kovalenko, A.; Ten-No, S.; Hirata, F. *J. Comput. Chem.* **1999**, *20*, 928.
(62) Pettersen, E. F.; Goddard, T. D.; Huang, C. C.; Couch, G. S.; Greenblatt, D. M.; Meng, E. C.; Ferrin, T. E. *J. Comput. Chem.* **2004**, *25*, 1605.